# Nonequilibrium Capture Rates Induce Protein Accumulation and Enhanced Adsorption to Solid-State Nanopores

**Kevin J. Freedman,*,† Syed Raza Haq,‡ Michael R. Fletcher,§ Joe P. Foley,§ Per Jemth,‡ Joshua B. Edel,† and Min Jun Kim*,⊥**

†Department of Chemistry, Imperial College London, South Kensington, SW7 2AZ London, United Kingdom, ‡Department of Medical Biochemistry and Microbiology, Uppsala University, Uppsala, Sweden, and §Department of Chemistry and ⊥Department of Mechanical Engineering and Mechanics, Drexel University, Philadelphia, Pennsylvania 19104, United States

**ABSTRACT** Single molecule capturing of analytes using an electrically biased nanopore is the fundamental mechanism in which nearly all nanopore experiments are conducted. With pore dimensions being on the order of a single molecule, the spatial zone of sensing only contains approximately a zeptoliter of volume. As a result, nanopores offer high precision sensing within the pore but provide little to no information about the analytes outside the pore. In this study, we use capture frequency and rate balance theory to predict and study the accumulation of proteins at the entrance to the pore. Protein accumulation is found to have positive attributes such as capture rate enhancement over time but can additionally lead to negative effects such as long-term blockages typically attributed to protein adsorption on the surface of the pore. Working with the folded and unfolded states of the protein domain PDZ2 from SAP97, we show that applying short (*e.g.*, 3−25 s in duration) positive voltage pulses, rather than a constant voltage, can prevent long-term current blockades (*i.e.*, adsorption events). By showing that the concentration of proteins around the pore can be controlled in real time using modified voltage protocols, new experiments can be explored which study the role of concentration on single molecular kinetics including protein aggregation, folding, and protein binding.

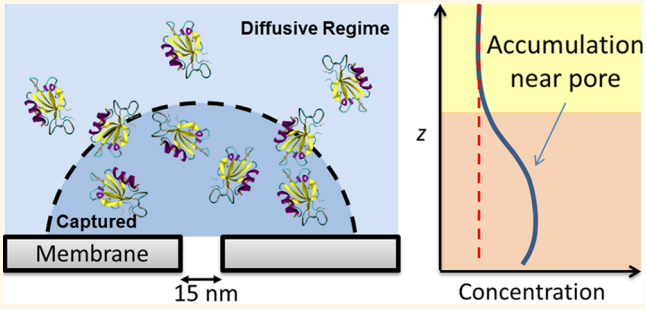


**KEYWORDS:** nanopores · capture rate · protein adsorption · biosensors · protein kinetics · energy barrier

The operating principles of nanopore sensing are conceptually simple: briefly, a solitary hole is drilled in a thin, nanometer-scale membrane and placed inside a fluidic cell wherein the pore is the only conduit for molecular or ionic transport.[1] Information is acquired about the molecules in one or both chambers when they transition from one side of the pore to the other in a process known as translocation. With the current state of technology, the information gained from nanopores includes the protein's size and charge,[2] excluded volume,[3] shape,[4] binding rate constants ($k_{on}$, $k_{off}$),[5] and binding state.[6−8] The frequency in which the molecule enters the pore is referred to as the capture rate and depends on the properties of the protein (*e.g.*, charge, size), the buffering solution (*e.g.*, pH, electrolyte concentration), the pore dimensions (*i.e.*, diameter and membrane thickness), and the voltage being applied across the pore.[9] Molecular capturing using a nanopore has mainly been described experimentally and mathematically using DNA,[9−13] with several protein studies coming out only more recently.[14,15]

Emerging from a field focused on DNA analysis and sequencing,[16] studies using nanopores have been increasingly focused on the kinetics and dynamics of proteins,[5,15,17−25] protein−protein complexes,[6,8] RNA−antibody complexes,[26] DNA−protein complexes,[23,27] and other molecular assemblies. Nanopores themselves have also become more complex with experiments now using biofriendly coatings (*i.e.*, lipids or self-assembling monolayers) on solid-state pores[8,28,29] and directed evolution

* Address correspondence to mkim@coe.drexel.edu, k.freedman@imperial.ac.uk.

Received for review July 28, 2014 and accepted November 14, 2014.

**Published online November 26, 2014**
**10.1021/nn5062645**

on biological pores.[30] A unique advantage of nanopore sensing is in the potential to acquire single molecule label-free, in-solution measurements.[31] This ultimately opens the door for numerous discoveries to be made including, as will be described, the thermodynamics of proteins. Typical bulk measurements average out the small-scale fluctuations that occur as a result of thermal energy; however, single molecule data can provide insight into these minute perturbations.[32] More important than this is the heterogeneity of a protein which is only now starting to be revealed through single molecule techniques.[33] A protein can be modified, mutated, or intrinsically have a multitude of different states which are in constant fluctuation.[34−37] When an ensemble average is taken, for example, of a structurally dynamic protein, the distinct differences between subpopulations become hidden and may not accurately represent any of the populations being averaged.

Major difficulties that are common to both solid-state and biological pores is that the molecular kinetics inside the pore may be altered by confinement effects, interactions with the pore, as well as the high electric field strengths present inside the pore. Some have solved the latter issue by collecting translocation data at a range of voltages and extrapolating biophysical properties to where the voltage is zero.[5] This is particularly useful when one is trying to compare the single molecule data obtained by nanopores to bulk properties such as binding constants. Confinement effects and nonspecific interactions with the pore are far less predictable; however, some studies have helped elucidate how these factors influence the translocation process for certain proteins.[18,38] Sexton *et al.* describes a conceptual framework for nonspecific interactions where proteins can either make multiple collisions with the pore not resulting in adsorption or alternatively can adsorb to the surface resulting in what are generally called long-term events.[38,39] Although coatings such as with lipids, antibodies, and chemical modifications can change the probability of a collision resulting in a long-term event, the effect of collisions and how they can be minimized has yet to be determined.

Proteins are complex molecules to study using nanopores. The difficulty is due to the fact that proteins have a heterogeneous charge distribution along its linear sequence as well as a varying level of charge and hydrophobicity on the surface of the folded protein. In comparison, double-stranded DNA has been a relatively ideal analyte as it can be designed to virtually any length and the backbone of the polymer has a homogeneous negative charge.[40−42] The long length of DNA makes it extremely unlikely that a second DNA molecule will enter the pore especially if the pore is plugged end-to-end with DNA, whereas proteins are typically small enough that multiple proteins can reside inside the pore at a given time, causing multiple steady current levels to be recorded. Since DNA has a homogeneous negative charge, electrostatic repulsion between the joined monomers while inside the pore does not occur. Interestingly, proteins have been shown to be quite unstable inside the pore due to the repulsion of opposite charges.[4]

In spite of these difficulties, there have been significant discoveries made by studying proteins with both biological and solid-state nanopores.[2,4,5,8,14,15,39,43−45] To do this, typically one must fine-tune experimental conditions to minimize the adsorption of proteins to the pore. Since keeping the pore free of protein is essential to collecting data, characterizing and perhaps even predicting when adsorption is likely to occur is critical to future success in the field of nanopore sensing. In this work, we describe how the interplay of diffusive and barrier-limiting capture kinetics can lead to protein accumulation around the entrance of the pore owing to an imbalance of the two rate equations. Using both the folded and unfolded state of our model protein domain (PDZ2), the energetic barrier height to cross the pore was calculated and the exponential barrier-limited regime was characterized. Most importantly, by showing that pore clogging can be abolished by reducing protein accumulation at the pore using shorter recording times (*i.e.*, voltage cycles), our study provides evidence that protein adsorption to the pore is initiated by simultaneous pore entry attempts (*i.e.*, steric frustration) by more than one protein and not necessarily by the protein's propensity to adsorb onto the pore wall as previously thought.

## RESULTS AND DISCUSSION

**Theory and Simulations.** The diffusion-based capture mechanism describes the process of a molecule transitioning from a spatial region away from the pore with low voltage-mediated displacement (*i.e.*, diffusion-dominated) to a hemispherical region around the pore where the molecule undergoes biased motion. In this case, biased motion refers to the molecule being driven by the electric field (*i.e.*, voltage-dominated) created when an applied voltage is applied across the membrane. The voltage profile that is created funnels the analyte from the bulk solution into the vicinity of the pore. Since the gradient of the voltage becomes greater in magnitude as a molecule approaches the pore, the velocity of the molecule increases by the function $v = \mu\nabla V(r)$, where $\mu$ is the electrophoretic mobility of the analyte. The applied voltage in which the charged protein overcomes Brownian motion is determined by $V_o = k_BT/ze$, where $z$ is the effective charge on the molecule, $k_B$ is the Boltzmann constant, $T$ is temperature, and $e$ is the elemental charge. The equation for the (concentration-normalized)

diffusion-based capture rate ($R_{diff}$ [$min^{-1}$ $nM^{-1}$]) is given by[9]

$$R_{diff} = \frac{\pi d^2 \mu}{4l} \Delta V$$

where $d$ is the diameter of the pore and $l$ is the length of the pore.

The second method in which the translocation process is described is through a Van't Hoff–Arrhenius law wherein the rate of translocation is determined by the energy barrier within the pore. The delivery of the analyte is necessary but not sufficient to result in translocation but rather the analyte waits until it has enough energy to climb the energetic barrier and enter the pore. The energetic cost in this case is mainly entropic, stemming from the restriction of motion within the nanopore. In the case of DNA, the threading probability is often used to derive the observed translocation rate. For proteins, we use a more general form of the equation which is given by[12]

$$R_{bar} = \omega \exp\left[\frac{(q\Delta V - U^{\ddagger})}{k_B T}\right]$$

where $q$ is roughly associated with the charge of the protein and $U^{\ddagger}$ is the energy barrier height without any voltage applied. Here, $\omega$ is generally interpreted as a molecule translocation attempt rate where not all attempts lead to a successful translocation event. Although $q$ has units of charge, we use it here as a relative value which defines the transport properties of the molecule inside the pore.

Based on the formulations of the diffusion ($R_{diff}$) and energy barrier ($R_{bar}$) capture rates, if $R_{diff} > R_{bar}$, proteins would be brought to the entrance of the pore faster than they could overcome the entrance barrier to translocate. The result would be that the local concentration around the pore would be enhanced (Figure 1a,b). Plotting the translocation frequency as a function of voltage would yield an exponential curve consistent with the expression for energy-barrier-controlled capture rate (*i.e.*, the limiting rate). If $R_{diff} < R_{bar}$, a protein would still be captured by the hemispherical region dictated by the voltage and pore dimensions; however, the protein would almost immediately be shuttled across the pore with little to no protein accumulation. In this scenario, plotting the translocation frequency as a function of voltage would produce a linear curve predicted by the diffusion-based capture mechanism.

By inspecting the above rate equations, there are three scenarios which are possible for a given set of experimental conditions. The first describes diffusion as the limiting rate giving rise to a linear capture rate function with respect to voltage. In the second scenario, the energy barrier rate is the limiting rate, yielding an exponential curve with respect to voltage. The last possibility is that the curves intersect, creating a piecewise function which changes from an exponential curve to a linear curve. This occurs at a point where molecules are brought to the pore at exactly the same rate as they are translocated ($R_{diff} = R_{bar}$). Using characteristic protein/pore properties, these three scenarios are shown graphically in the Supporting Information (Figure S1). In the case where $R_{diff} > R_{bar}$, the rate of accumulation is the difference between the two rates. The accumulation of proteins at the entrance of the pore can therefore be expressed by the following:

$$R_{acc}\left[\frac{\text{molecules}}{\text{min}}\right] = C(R_{diff} - R_{bar}) = \frac{C_{bulk}\pi d^2 \mu}{4l}\Delta V - \omega C_{captured}(t)\exp\left(\frac{qV - U^{\ddagger}}{k_B T}\right)$$

where $C$ is concentration. Since there exists potentially two regimes of concentration, subscripts are used to indicate which concentration regime should be considered ($C_{bulk}$ *versus* $C_{captured}$). Far away from the pore, the capture of molecules *via* diffusion will depend mostly on the bulk concentration of the protein. Assuming that the translocation success rate is constant (defined as the rate at which molecules pass through the pore divided by the attempt rate, $\omega$), a larger number of proteins around the pore will enhance the barrier-limiting rate. $C_{captured}$ is therefore the concentration at the pore's entrance which increases over time when $R_{diff} > R_{bar}$. Enhancement of $C_{captured}$ is expected to increase the translocation rate both by increasing the number of molecules which have enough energy to cross a fixed energy barrier height as well as by decreasing the energy barrier due to a greater concentration gradient across the membrane.

After the initial moments of applying a voltage, $C_{captured} = C_{bulk}$ and the individual capture rates are constant. It follows that the rate of accumulation is also fixed, and therefore, the number of molecules close to the pore linearly increases with time. This of course assumes that the rate of escape from the vicinity of the pore *via* diffusion is minimal; however, based on the definition of the capture radius, we can theoretically assume this to be accurate. The rate of accumulation changes with voltage, as shown in Figure 1d. The parabolic nature of the curve suggests that accumulation at the pore can be reduced by either reducing or increasing the applied voltage. In this model, we also see that the rate of accumulation decreases when the energy barrier is reduced to a lower energy level, as expected. Although finding the right conditions for accumulation to occur strictly depends on the analyte molecule, the pore geometry is an essential component which was modeled using finite element analysis. As the aspect ratio of the pore decreases, the potential drop outside of the pore becomes more prominent (Figure 1e). As a result, the capture radius of the pore and the number of molecules inside the capture radius increase (Figure 1f,g). These graphs indicate that the same capture radius and potential distribution can be

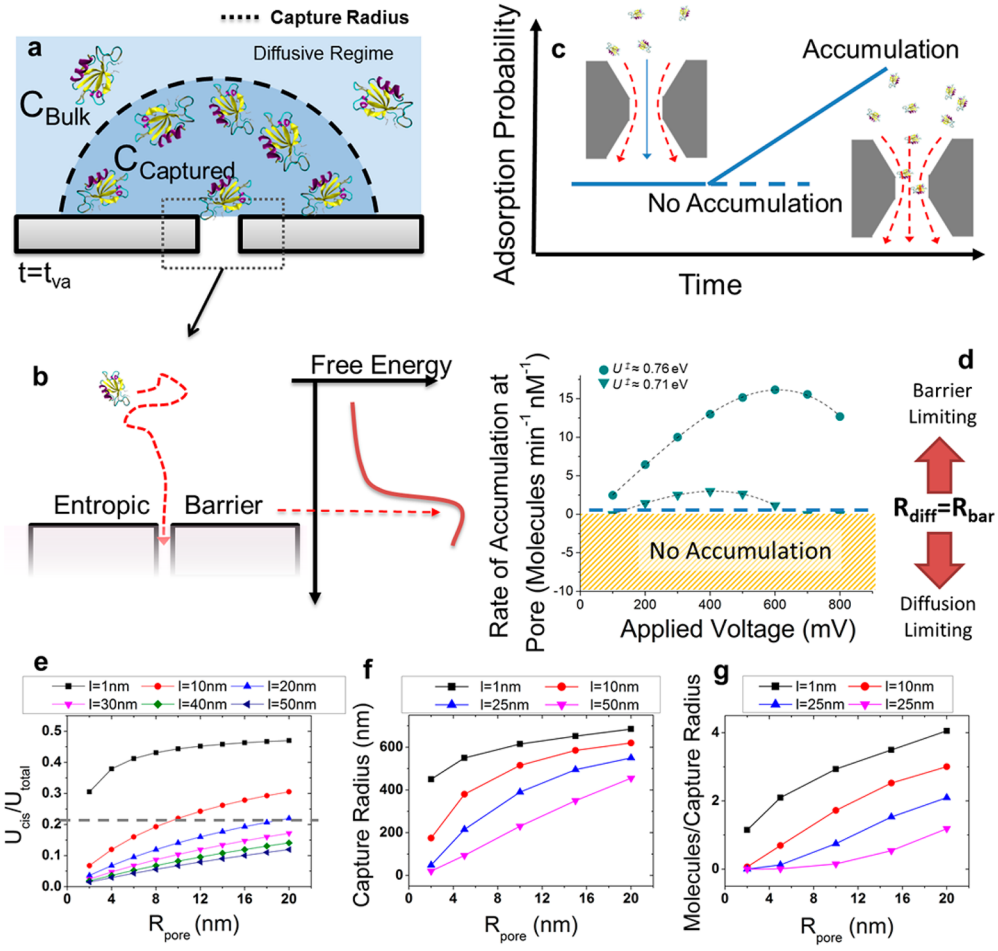


**Figure 1. (a) Schematic representation of the nanopore (under $R_{diff} > R_{bar}$ conditions) with the dotted line representing the capture radius for proteins. The concentrations of the bulk protein solution ($C_{bulk}$) and of the area within the capture radius ($C_{captured}$) are labeled. (b) Schematic representation of the free energy *versus* the spatial location of the protein as it approaches the pore. (c) Schematic representation the proposed nanopore adsorption model. Dotted red lines indicate a higher probability of adsorption. (d) Rate of accumulation plotted with respect to applied voltage. Values were obtained by analytically solving the rate equations with characteristic protein and pore values ($D_{diff} \approx 10^{-10}$ m$^2$/s, $q \approx +3$, $U^{\ddagger} \approx 0.76$ eV, $\mu \approx 1 \times 10^{-5}$ cm$^2$/Vs, $d_{pore} \approx 15$ nm, $l_{pore} \approx 50$ nm). (e) Finite element analysis of the potential drop at the entrance of the pore ($U_{pore}$) relative to the total potential drop ($U_{total}$) for various pore lengths ($l$ = 1, 10, 20, 30, 40, 50 nm); the dotted line represents pores with aspect ratios equal to 1. (f,g) Capture radius and the number of molecules inside the capture radius (assuming $V$ = 0) as a function of the pore diameter for various pore lengths ($l$ = 1, 10, 25, 50 nm).**

replicated using a wide range of geometries and membrane thicknesses, allowing one to control $R_{diff}$ (which only depends on the capture radius) while varying other parameters.

Grounded on the aforementioned theoretical framework, protein concentration enhancement at the entrance of the pore is the result of unequal rate equations. It has been shown using DNA analyes[9] that an increase in the bulk analyte concentration can be observed as an increase in the capture rate. Protein analytes, however, can become stuck within the pore, causing multilevel, long-term blockades. Key properties of the protein which determine the probability of sticking to the surface include the stability and net charge of the protein as well as the hydrophilicity and charge of the surface. A protein with a high degree of structural stability is less likely to adsorb to a surface since the free energy associated with adsorbing to the surface does not outweigh the free energy gained by changing conformation. Of course, hydrophobic and electrostatic interactions can aid in making adsorption energetically favorable or unfavorable depending on the surface−protein combination.[46]

The membrane composition in this experiment is $Si_3N_4$, which holds a slight negative charge. The zeta-potential and surface charge density at pH 7 is *ca.* −15 mV[47] and −0.02 C/m$^{-2}$, respectively.[48] Oxygen plasma treatment also renders the surface hydrophilic (see Materials and Methods for plasma dosage). Using sequence-based protein property tools, the charge of the PDZ molecule at pH 7 is +3.8*e*, the instability index is 17.34 (*i.e.*, stable), and the grand average of hydropathicity is −0.261 (*i.e.*, hydrophilic).[49] Two hydrophilic surfaces coming together is energetically unfavorable since dehydration incurs an energetic penalty. Therefore, the stability and hydrophilicity of the protein do

not favor adsorption, while electrostatic forces, albeit small in magnitude due to the low charge and high screening at 2 M KCl, contribute toward adsorption. When these factors are taken into consideration, PDZ2 is not an extreme case; it is neither overly adsorptive nor lacking the ability to adsorb. As a reference, bovine serum albumin (BSA) has an instability index of 40.28 (*i.e.*, unstable), a grand average of hydropathicity of −0.429 (*i.e.*, hydrophilic), and a charge of −9.9*e* at a pH of 7.[39]

In order for a protein to successfully adsorb to the pore's surface, the protein must first collide with the pore wall. In the literature, the leading adsorption-based model takes into account a single protein and its corresponding "sticking probability".[38] Based on the notion that (1) higher protein concentrations increase the rate of long-term current blockades and (2) the rate of accumulation is a linear function (*i.e.*, the difference between two capture rate equations), the adsorption probability for protein within a nanopore should be constant in the case of no accumulation and a linearly increasing function when $R_{diff} > R_{bar}$. The first notion is supported by the work by Niedzwiecki and colleagues,[39] who reported that only 2 out of 27 pores showed long-term events below 20 nM BSA, while 80% of pores showed long-term events at 180 nM BSA. This model predicts that adsorption can happen when a single protein enters the pore but also predicts that adsorption is enhanced when multiple proteins enter the pore (Figure 1c).

**Constant Voltage Recordings.** In order to validate our hypothesis about the existence of protein accumulation around the entrance of the pore, a member of the PDZ protein domain family was used, which is a highly conserved protein−protein interaction domain found within many organisms.[50] The exact sequence of the protein is that of the pseudo-wild-type SAP97 PDZ2 (here denoted PDZ2), which was expressed and purified as previously described.[51,52] PDZ2 is a relatively small protein domain (approximately 4 × 5 nm) with a low net positive charge (+3.8*e*) at neutral pH. Results were obtained using pores drilled with a field emission transmission electron microscope (JEOL 2100F) with a diameter of 15 ± 2 nm (50 nm thick membranes).

Upon adding a 10 nM concentration of PDZ2 to one side of our fluidic cell, transient current drops were detected within the first 5 min of recording. Events remained short and transient for the first 10 min until long-term current events were observed in a reproducible and time-dependent manner. The long-term events were arbitrarily defined as any event that lasted more than 0.5 s. Typically, these long-term events had the same current blockade depth as the transient events. Once the pore is in the blocked state, transient events can still be observed since the pore diameter is several times the size of a single protein molecule. After 10 min of applying a constant voltage, the blocked current further decreased in a stepwise manner,

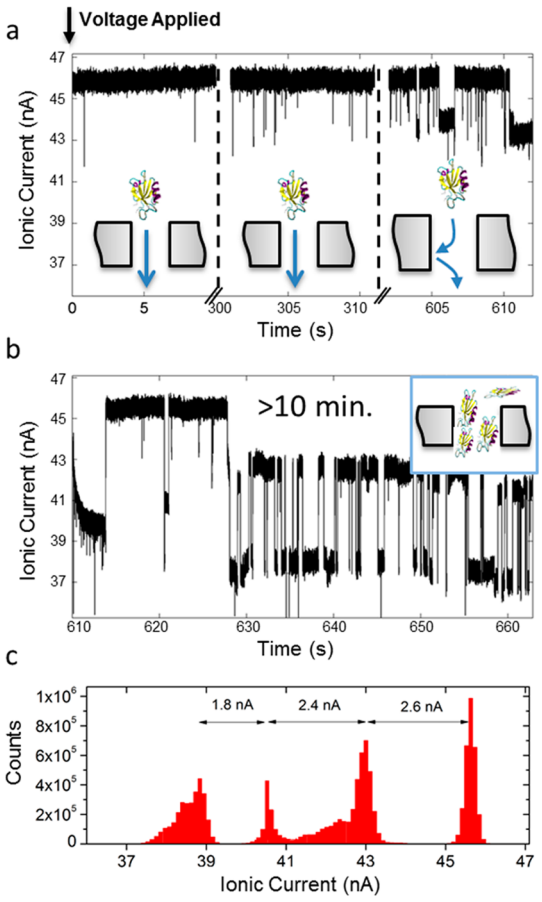


**Figure 2. (a) Ionic current recording 1, 5, and 10 min after applying a constant applied voltage (*V* = 500 mV). The time-dependent sensing of proteins was independently observed in four different pores. (b) After 10 min of applying a constant voltage, the current no longer has a steady baseline but rather resides in one of multiple blocked states of the pore. *Y*-axes in both plots are the same. (c) All-points histogram of the ionic current recording shown in (b) showing four stable levels of ionic current.**

consistent with the magnitude of the transient current drops. The quantized nature of the current level is consistent with proteins adsorbing/desorbing on the surface of the pore. These results are summarized in Figure 2, where ionic current traces are plotted 0, 5, 10, and >10 min after the initial application of 500 mV of voltage. To our knowledge, this is the first report of event frequency being time-dependent.

An all-points histogram, taken of an ionic current recording, is useful at identifying the multitude of potential states in which the pore is conducting ions. If there is more than one discrete state in ionic conductance, peaks in the histogram correspond to the number of proteins which exist inside the pore (Figure 2c). The peak with the largest current value is the open pore conductance corresponding to no protein residing inside the pore. The second peak is the blocked ionic current level corresponding to a single protein inside the pore. It should be noted that the long-term current blockade depth should not be interpreted in the same way as the current drop

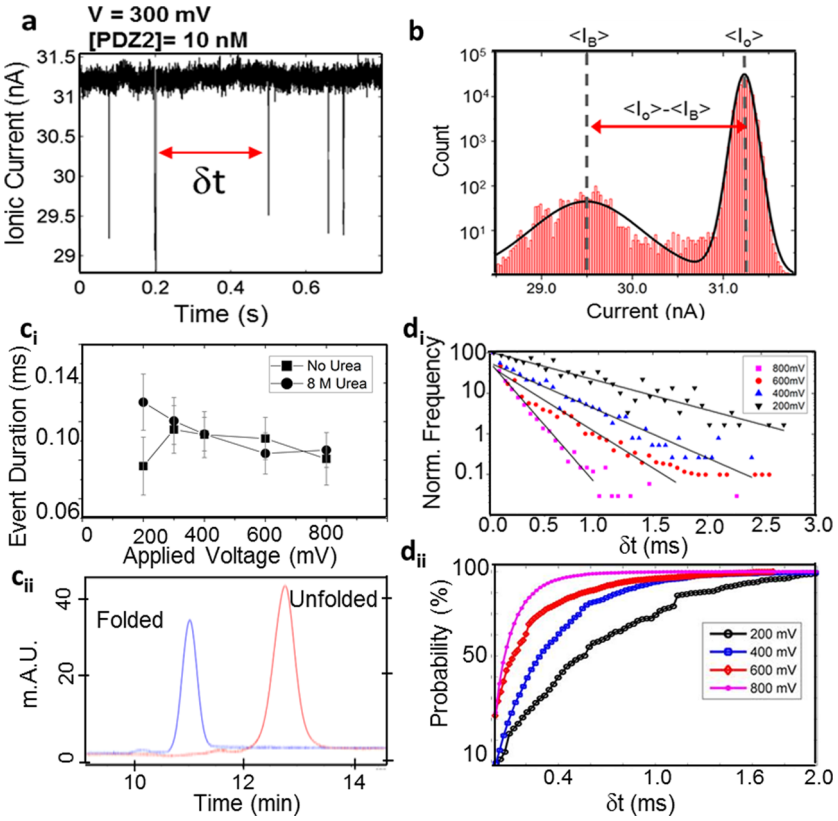


**Figure 3. Event analysis for constant voltage recordings. (a) A representative current trace showing two events separated by the inter-event time, $\delta t$. (b) An all-points histogram of the ionic current trace where the transiently blocked state and the open state of the pore are clearly observed. ($c_i$) Event durations for the folded (no urea) and unfolded states (8 M urea) of PDZ2 within the voltage range of 200−800 mV. Mean values were obtained through a least-squares fit of a single exponential to each data set. ($c_{ii}$) Capillary electrophoresis results for the folded and unfolded PDZ2. (d) Plots showing the inter-event time fitted to exponential functions (exponential decay value: 0.69 (200 mV), 0.22 (400 mV), 0.09 (600 mV), 0.07 (800 mV)) as well as displayed as Poisson cumulative distribution functions (cdf) at four voltages: 200 mV, 400 mV, 600 mV, 800 mV.**

parameter extracted from short events. This is due to the fact that the adsorbed state is not the same as the free-solution state of the protein. As a second protein enters the blocked pore, the current is further reduced. Interestingly, the change in current is not as great as the $\Delta I$ between the open pore and the first current blockade level. In fact, with each additional protein that enters the pore, the change in current decreases to a lower $\Delta I$. This was predicted through molecular dynamics simulations recently wherein one, two, and three proteins were placed inside the pore and the current drop was shown to be nonadditive.[53] Since no changes in structure were modeled in the above study, the decreasing $\Delta I$ could be due to varying protein positions within the pore or a manipulation of ion flow due to the introduction of charges on the surface of the pore.

**Event Detection and Analysis.** Protein translocation events, defined as transient decreases in current less than 500 ms, were detected using a threshold, and characterizing features were extracted including event duration and event amplitude. The threshold was typically set to 3−4 standard deviations away from the noise level of the open pore current at each voltage. Once events were detected, the interevent time, $\delta t$, was calculated as the time between the start of each event (Figure 3a). The event statistics were gathered from multiple recording sessions where each recording was typically under 5 min in duration.

If an all-points histrogram of the ionic current is plotted (Figure 3b), two prominent peaks are observed. The larger peak corresponds to the open pore current, and the second smaller peak characterizes the blocked state of the pore (*i.e.*, containing a single protein molecule). Typically, one can verify the existence of an energy barrier inside the pore by experimentally measuring the time it takes the protein to traverse the pore. If no energy barrier exists inside the pore, the event duration is expected to be inversely proportional to the applied voltage. Conversely, if an energy barrier exists, the event duration will show an exponential dependence with applied voltage. Plotting the event duration trend with voltage, however, assumes that the analyte keeps its structural and chemical properties the same no matter the magnitude of the voltage. Due to the range of voltages used in this study, plotting the event duration *versus* applied voltage (Figure 3$c_i$) instead provided evidence for protein unfolding through

electric-field-induced destabilization as described previously.[4] Briefly, as the applied voltage was increased from 200 to 300 mV, the originally natively folded protein is observed to have longer event durations despite the larger electrophoretic force. Another possible explanation for the increase in the event duration is if the voltage-mediated electro-osmotic flow inside the pore is opposing the electrophoretic force. In this case, however, since the protein is positively charged and the SiN membrane is negatively charged ($-0.02$ C m$^{-2}$), the protein translocates through the pore in the same direction as the electro-osmotic flow. Further study of the effects of electro-osmotic flow can be found in the work by Firnkes and colleagues.[47]

Although the effect of the energy barrier could not be directly observed in the event duration data, we aimed to explain the event durations based on the electrophoretic mobility of the folded and unfolded protein. In order to determine how the state of the protein would affect the electrophoretic mobility of the protein, capillary electrophoresis was performed on the natively folded protein and the unfolded protein. We found that the migration time for the unfolded PDZ2 molecule was significantly longer than that of the folded state. The electrophoretic mobilities, $\mu$, for the folded and unfolded PDZ2 protein were found to be $|\mu|_{\text{folded}} = 1.38 \pm 0.02 \times 10^{-5}$ cm$^2$/Vs and $|\mu|_{\text{unfolded}} = 1.02 \pm 0.05 \times 10^{-5}$ cm$^2$/Vs, respectively (electropherograms shown in Figure 3c$_{ii}$). The increase in event duration between 200 and 300 mV can therefore be explained in terms of a lower electrophoretic mobility due to unfolding. Previous work with this protein has shown that PDZ2 unfolds inside the pore as a result of the electric field pulling the positive and negative amino acids in opposing directions, thereby stretching the protein along a single axis.

The interevent time, $\delta t$, was calculated as the difference between the starting points of two sequential events. This was done for the voltage range of 200−800 mV with a voltage increment of 200 mV. The interevent time parameter forms a Poisson distribution with a variance that depends on the applied voltage. Despite this, the $\delta t$ parameter is typically shown on a log scale and fit with an exponential (Figure 3d$_i$). Since the probability of observing two simultaneous events is extremely small, the same data can also be displayed as a cumulative Poisson distribution function which shows the changes between voltages most clearly while still showing a small probability of simultaneous events (Figure 3d$_{ii}$). With an applied voltage of 200 mV, the interevent time distribution has a large variance compared to the 800 mV condition. At 800 mV, the probability of obtaining an interevent time greater than 1.5 ms is extremely low (<1%). Additional event property histograms are supplied in the Supporting Information.

**Capture Rates for the Folded and Unfolded Protein.** Capture rates were calculated by counting the number of events per unit time and normalizing by the concentration of protein. Capture rates could also be calculated by using fitting parameters of the $\delta t$ distribution. Using the first method allowed us to detect any traces of capture rate enhancement over time which would be hidden when all the data are merged to form the $\delta t$ distribution. Measurement times were typically under 30 s and, as we will show later, insignificant amounts of protein accumulation occurred within this short window of time. Therefore, assuming a pseudo-steady state with no capture rate enhancement, we tested three experimental conditions in order to study the capture kinetics of proteins as a function of the applied voltage: (1) 0 M urea in both cis and trans chambers, (2) 8 M urea in cis chamber and 0 M urea in the trans chamber, and (3) 8 M urea in both the cis and trans chambers. The capture rates for all three conditions start out having an exponential dependence, which means that proteins are arriving at the pore and then wait to have enough energy to cross the pore. Interestingly, in the 0 M urea condition, there is both a barrier-dominated regime and a linear diffusive regime (Figure 4a). The data collected at 0 M urea show the unique transition from $R_{\text{diff}} > R_{\text{bar}}$ (200−600 mV) to $R_{\text{diff}} < R_{\text{bar}}$ (600−800 mV). The $R_{\text{diff}} < R_{\text{bar}}$ condition is favorable because the capture rate is high and protein accumulation does not occur. We observe no long-term current blockades in this voltage range with the folded protein.

In both the urea conditions, a transition into a linear capture rate is not observed. The diffusive capture rate depends on the state of the protein through the electrophoretic mobility term, $\mu$. However, the energy barrier rate equation is exponentially dependent on the size of the barrier height. The unfolded state of the protein will have a significantly larger energy barrier to transition into a confined space since its hydrodynamic radius is larger, and it will have a greater number of conformational states available to it outside the pore. Although both rate equations will become smaller, the energy barrier capture rate ($R_{\text{bar}}$) will be more drastically reduced and will be the limiting rate throughout the voltage range tested.

Using well-established techniques, the energy barrier for the folded and unfolded protein can be calculated based on the capture data and the pore geometry. To do this, the capture rate is redefined as $R = kv \exp((U^{\ddagger} - \Delta U)/(k_B T))$ where $k$ is a probability factor, $v$ is the frequency factor, $U^{\ddagger}$ is the activation energy or barrier height, and $\Delta U$ is the reduction in the energy barrier due to the applied potential.[12] In order to obtain an estimate of the frequency factor, a barrier penetration calculation is performed where $v = CD_{\text{diff}}A_{\text{pore}}/l_{\text{pore}}$. Using $C = 6.023 \times 10^{18}$ molecules/m$^3$, $D_{\text{diff}} = 10^{-10}$ m$^2$/s, $A_{\text{pore}} = 1.77 \times 10^{-16}$ m$^2$, and $l_{\text{pore}} = 50$ nm, the value of

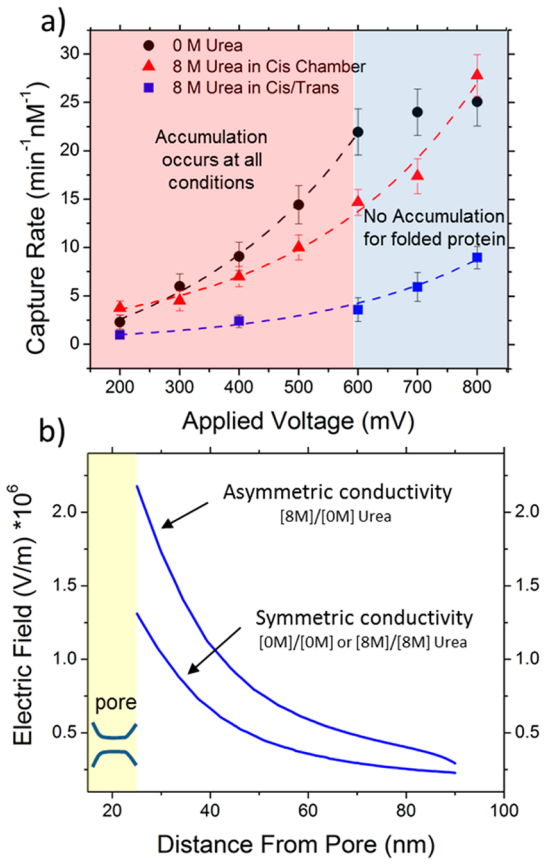


**Figure 4. (a) Capture rates for three experimental conditions as a function of voltage (200−800 mV). Solution conditions include 0 M urea in both sides of the flow cell (black circles), 8 M urea in the cis chamber only (red triangles), and 8 M urea in both chambers (blue squares). All experiments were conducted with a 15 nm pore, 2 M KCl, and with the PDZ2 protein domain (all experiments performed at [PDZ2] = 10 nM with the exception of the asymmetric condition which was at [PDZ2] = 100 nM). A minimum of 400 events was used for each data point (exact event counts are listed in the Materials and Methods). (b) Electric field distribution on the cis side of the flow cell under symmetric (0 M urea/0 M urea) and asymmetric (8 M urea/0 M urea) conductivity conditions. The urea concentrations were simulated as a change in solution conductivity which was measured experimentally to be 112 and 200 mS/cm for 8 and 0 M urea, respectively.**

the energy barrier for the folded state of the protein was $U^{\ddagger} \approx 1.9\ k_BT$. Performing a similar calculation for the unfolded state of the protein yielded $U^{\ddagger} \approx 3.3\ k_BT$. In comparison, a similar study found the energy barrier for folded maltose binding protein (MBP) to be ~7.4 and 10.4 $k_BT$ for the unfolded protein.[15] The smaller absolute value of the energy barrier in this study is likely due to the size of the protein relative to the pore. In this work, the average diameter of the protein can be estimated to be ~2.5 nm, which was studied using a 15 nm pore, whereas MBP is nearly twice this size and studied using a 20 nm pore. The relative size of the pore is larger in this study, which means the confinement effects on the protein are less.

The asymmetric condition where 8 M urea was put into only one side of the flow cell increased the capture rate through electrostatic focusing of proteins. Typically, electrostatic focusing occurs when asymmetric salt concentrations are used on either side of the membrane as previously shown with DNA analytes.[9] Here, we show that electrostatic focusing also works using proteins and asymmetric concentrations of urea which also alters the solution conductivity. Conductivity measurements of 2 M KCl with and without 8 M urea were 112 and 200 mS/cm, respectively. To explain the capture enhancement briefly, the electrical circuit under asymmetric conditions can be thought of as three resistors in series ($R_{KCl\text{-}cis}$, $R_{pore}$, $R_{KCl\text{-}trans}$). The lower conductivity solution in the cis chamber (*i.e.*, containing urea) causes a redistribution of voltage that depends on the degree of asymmetry. The net effect is a higher electric field that emanates from the pore and is able to capture a greater number of molecules. Numerical simulations of the electric field enhancement can be viewed in Figure 4b. The higher electric field strength on the side of the pore with proteins amounts to both $R_{diff}$ and $R_{bar}$ increasing. It should also be noted that the energy barrier for the condition where urea is only in the cis chamber is the same as the energy barrier when urea is in both chambers. The change in the capture rate is a direct consequence of the modulation of the electric field distribution, not the energy barrier at the pore.

In the first few minutes of applying a voltage, we observed insignificant changes in the capture rate since the concentration of the protein immediately outside the pore takes time to increase (event counts per cycle shown in Figure 5d). We predict that there is a threshold concentration that is reached which makes interactions with the pore increasingly probable. If the voltage at which the protein overcomes Brownian motion is determined by $V_o = k_BT/ze$ and we solve for the voltage profile assuming a 15 nm pore and an ion screened protein charge of $+1.9e$ (assuming 50% charge screening),[54] the capture radius around the pore is $r^* \approx 121$ nm at 200 mV. Given that a protein is captured and is trapped by the voltage potential $V(r)$, it will spend most of its time a distance $r_g$ away from the pore, where $r_g$ is the protein's radius of gyration (nm). The difference between $r^*$ and $r_g$ will determine how long it takes to reach the threshold concentration. Since the unfolded protein has a larger $r_g$, we expect the unfolded protein to stay further away from the pore while waiting to cross the energy barrier of the pore. In addition to the larger energy barrier to cross the pore, the unfolded protein may also have a reduced capture rate as a result of its greater distance away from the pore. We approximated the radius of gyration using equations in the literature yielding an $r_g \approx 1.38$ nm for the folded state and $r_g \approx 2.1$ nm for the unfolded state, which coincide with proteins with a similar number of amino acids.[55,56]

**Effect of Protein Accumulation.** Protein adsorption onto the pore surface is an adverse consequence of the

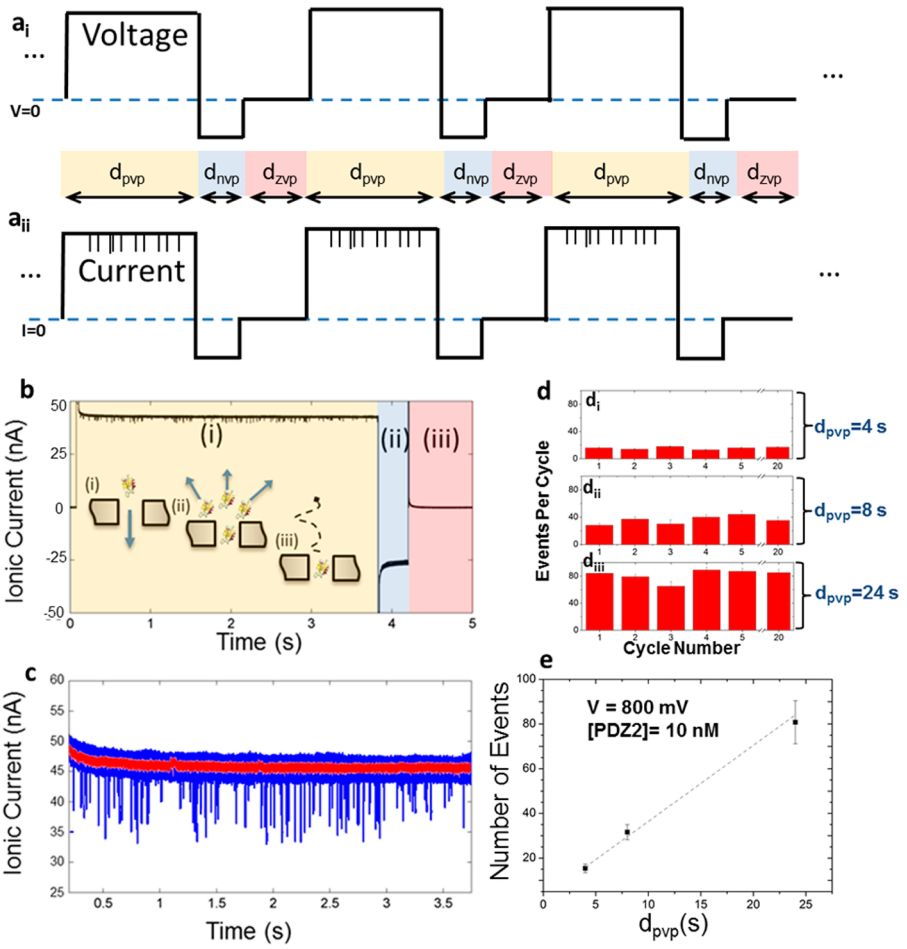


**Figure 5. (a) Schematic representation of the voltage cycles used to translocate proteins through the nanopore as well as the resulting current response. The durations of the positive voltage pulse ($d_{pvp}$), negative voltage pulse ($d_{nvp}$), and the zero voltage pulse ($d_{zvp}$) are defined as shown in the schematic. (b) Three-stage voltage stepping protocol: (i) record mode, (ii) unclogging mode, (iii) rerandomization mode. (c) Overlay of 30 current traces showing a stable baseline current and only short transient events. The 30 traces were taken from a recording that was running for >10 min. The red trace is the baseline current of a single trace. (d) Number of events per cycle at 800 mV and a protein concentration of 10 nM. The duration of the positive voltage pulse ($d_{pvp}$) that was used here had the following values: 4 s ($d_i$), 8 s ($d_{ii}$), 24 s ($d_{iii}$). A set of 20 cycles was performed three times, and the average for each cycle number was calculated. (e) Average number of events plotted as a function of cycle duration (s) for a protein concentration of 10 nM and an applied voltage of 800 mV.**

protein coming into close proximity with a solid-state surface. Under normal circumstances, one would have to modify the surface of the pore with an antifouling agent to prevent long-term events from occurring. Surface modifications, however, increase nanopore preparation time and reduce device yield due to unintentional blocking of the pore. The reproducibility of surface modifications is also typically low, which can cause error across experiments. With unmodified pores, proteins can adsorb onto the surface of the nanopore; however, this work suggests that the adsorption process is coerced through protein accumulation at the pore entrance.

In order to show that protein accumulation is the cause of long-term events and not time-dependent dimer formation, which may also block the pore for longer time periods, a protocol was developed which would limit the duration of a constant applied voltage. A three-step voltage stepping protocol was developed for this purpose (Figure 5a). The first ~3.5 s is the "record" mode in which useful data were recorded followed by an unclogging step (0.5 s in duration) and a zero voltage step (1 s in duration) to allow proteins to rerandomize *via* diffusion. A second reason for the zero voltage steps was that, qualitatively, it was noticed that zero voltage unclogged the pore faster than a sudden negative voltage. Previous reports by Niedzwiecki and colleagues show that the blocked state of the pore becomes more probable at higher voltages.[39] The duration of the positive voltage pulse ($d_{pvp}$) (*i.e.*, the "recording" mode) was varied between 4 and 24 s to determine if there was any time dependence to event frequency. The linear increase in the number of events per cycle with cycle duration implies that there is no significant enhancement of the capture rate within these time scales (Figure 5d,e). Using the modified voltage protocol on the same solution as before (10 nM PDZ2) yielded no long-term current blockades

(Figure 5c; overlay of 30 traces taken 30 min after initiating the recording). The fact that the voltage cycling protocol was successful at preventing long-term events suggests that adsorption is a controllable process within the nanopore. If adsorption was solely due to a single protein colliding with the pore wall, the probability of observing a long-term event would have been the same. When studying PDZ2 with different pores within this study, virtually no modification of the protocol was necessary. We expect modifications would be needed when changing the protein and pore size; however, this can be done within the first few minutes of an experiment.

By applying transient voltage pulses, we showed that long-term events can be avoided provided that $R_{diff} > R_{bar}$. An alternative method to prevent long-term events is to make use of electrostatic focusing which enhances $R_{bar}$ relatively more compared to $R_{diff}$ since the $\Delta V$ term is an exponential function. In this study, we observe a change in the limiting rate equation at 600 mV for the folded state of the protein. Using electrostatic focusing, the voltage at which $R_{diff}$ intersects $R_{bar}$ can be manipulated. Using exponential and linear curves to fit the experimental data as a function of $\Delta V$, we show that a 10 and 50% enhancement in the electric field through asymmetric salt conditions can reduce the voltage where protein accumulation first starts to occur from 600 to 400 mV (Supporting Information).

This work has shown that long-term current blockages are not solely caused by a protein's susceptibility to stick to the pore but rather that accumulation at the pore's entrance also plays an important and, perhaps, a dominant role. The significance of this work also extends to the kinetics of single molecules since crowding has been shown to substantially affect binding,[57,58] oligomerization,[57,59] and protein folding.[58,60−62] In theory, nanopores could be used to study the effects of protein crowding (*i.e.*, enhancements of certain states or rare protein−protein complexes) in real time. The known stabilizing effects of higher solute concentrations is well-documented; however, it is unclear how long these effects can be observed after removal from such an environment. Nanopores may be able to answer this question since a single protein must leave the crowded environment and enter the pore. Modifying the voltage across the membrane can alter the translocation time and therefore probe the molecule at various time points. Protein accumulation could also enhance the existence of rare protein states immediately before sensing them. In terms of protein binding and oligomerization, protein crowding is important to consider since protein complexes could be formed that are larger than the pore, causing another source of long-term current blockades. If two proteins can be shown to accumulate at different rates, the measurement of protein binding kinetics may also be obtainable. This study provides additional evidence that nanopores do not measure bulk solution properties of an analyte which has otherwise been shown by previous experiments.[5,27,47,48]

## CONCLUSION

In this report we show that the rate in which proteins translocate a solid-state pore is not constant with time. Instead, event frequency is enhanced over time through a process involving protein accumulation, which stems from unbalanced rate equations. Protein accumulation is potentially useful as it can enhance the frequency of events when using ultralow protein concentrations; however, we also observe a greater probability of long-term events at our specific experimental conditions. Event frequency was plotted as a function of voltage between the range of 200 and 800 mV for both the folded and unfolded state of the protein. We discovered that at high voltages (600−800 mV) the folded protein, which has a lower energy barrier, is no longer limited by the barrier translocation rate (*i.e.*, no longer the rate-limiting step). To our knowledge, this is the first time observing a transition between barrier-limited and diffusion-limited translocation kinetics. By knowing the limiting rate function, we can identify protein crowding in translocation data and steps to control it can be taken. In this work, a modified voltage protocol was developed which allows the enhanced concentration of proteins around the pore to diffuse away. Ultimately, this led to a steady baseline and longer data collection time. The broad significance of this work includes redefining the way in which proteins cause long-term current blockades. Previously, it was thought that long-term events were caused by the proteins' propensity to adsorb to the pore, whereas here it is clear that accumulation at the pore also plays a role. Furthermore, local concentration enhancement is shown to be controllable and potentially useful for studying concentration-dependent processes such as aggregation, folding, adsorption, and protein−protein binding.

## MATERIALS AND METHODS

**Protein Expression, Purification, and Equilibrium Denaturation.** SAP97 PDZ2 was expressed and purified as described previously.[51,52] The purity of the proteins was checked by SDS-PAGE and their identity by mass spectrometry. The protein data bank code for the pseudo-wild-type SAP97 PDZ2 protein domain is 2X7Z. The sequence is given by the one letter amino acid code as follows: MHHHHHLVPRGSKPVSEKIMEIKLIKGPKG-LGFSIAGGVGNQHWPGDNSIYVTKIIEGGAAHKDGKLQIGDKLLAV-NNVALEEVTHEEAVTALKNTSDFVYLKVAKPTS.

**Fabrication.** Nanopores were drilled in a 50 nm thick free-standing silicon nitride membrane which was supported on all sides by a silicon chip. Fabrication of this membrane consisted of first depositing a layer of low-stress silicon nitride on a silicon wafer using low-pressure chemical vapor deposition followed by photolithography, deep reactive ion etching, and KOH etching to form a $50 \times 50\ \mu m^2$ square membrane. Pores were then drilled using a field emission TEM (JEOL 2010F), forming pores with diameters of $15 \pm 2$ nm. Prior to single molecule experiments, the nanopore was treated with oxygen plasma for 10 min (12 W power).

**Single Channel Recordings.** Three nanopore chips were prepared and used during this study. Pore characterization and event recording was accomplished by placing the nanopore between two electrolytic half-cells filled with buffered potassium chloride (2 M KCl). The nanopore chip was held in place using a custom-built polycarbonate flow cell with polydimethylsilane gaskets to ensure that the only path of ionic current is through the nanopore. Electrodes (Ag/AgCl) were placed in both chambers and connected to the headstage of a patch clamp amplifier (Axopatch 200B, Molecular Devices Inc.), which allowed the ionic current to be measured at various applied voltages. Signals were recorded at 250 kHz with a low-pass Bessel filter of 10 kHz. Conductance measurements were performed prior to each experiment and were found to be within 5% of each other. A graphical representation of our custom-built flow cell used for all experiments, a TEM image of a 15 nm pore, and *IV* curve graphs for several pores are shown in the Supporting Information.

**Data Acquisition and Analysis.** Prior to each experiment, protein solutions were made fresh by diluting the desired protein into buffered KCl for a final protein concentration of 10 nM (diluted in 2 M KCl, 10 mM potassium phosphate buffer, pH 7). After characterization of the pore, protein was injected into one chamber of the flow cell, while a constant voltage is applied across the pore. Protein translocation events, defined as transient decreases in current, were detected using a threshold, and characterizing features were extracted including event duration and event amplitude. Event detection was performed using custom Matlab scripts. Event durations were calculated by using the width of the event halfway between the baseline current value and the maximum current drop value. The reported values for event duration were obtained by fitting the binned data with a single exponential function. All other event or capture rate statistics were obtained by Gaussian and exponential fits of histograms using Origin 8.1. The number of events used for the capture rate analysis are as follows: (1) 0 M/0 M urea: 589 (100 mV), 849 (200 mV), 923 (300 mV), 1029 (400 mV), 405 (500 mV), 659 (600 mV), 705 (700 mV), 759 (800 mV); (2) 0 M/8 M urea: 488 (100 mV), 691 (200 mV), 501 (300 mV), 576 (400 mV), 874 (500 mV), 493 (600 mV), 749 (700 mV), 1032 (800 mV); (3) 8 M/8 M urea: 780 (200 mV), 843 (400 mV), 687 (600 mV), 1034 (800 mV).

*Conflict of Interest:* The authors declare no competing financial interest.

*Acknowledgment.* This material is based upon work supported by the HFSP young investigator award (RGY0075/2009-C). This work was also in part supported by the NSF (CMMI #1435000). K.J.F. acknowledges the NSF Graduate Research Fellowship under Grant ID No. 2010095296 and the IIE's Whitaker International Program. J.B.E. acknowledges the receipt of an ERC starting investigator grant as well as BBSRC. Finally, P.J. acknowledges a grant from the Swedish Research Council.

*Supporting Information Available:* Modeling capture rate curves, preventing protein crowding using asymmetric conductivity, capillary electrophoresis data, current traces as a function of voltage, event histograms, current traces for the unfolded state, and data collected for the unfolded protein using voltage cycles. This material is available free of charge *via* the Internet at http://pubs.acs.org.

## REFERENCES AND NOTES

1. Li, J.; Stein, D.; McMullan, C.; Branton, D.; Aziz, M.; Golovchenko, J. Ion-Beam Sculpting at Nanometre Length Scales. *Nature* **2001**, *412*, 166–169.
2. Fologea, D.; Ledden, B.; McNabb, D.; Li, J. Electrical Characterization of Protein Molecules by a Solid-State Nanopore. *Appl. Phys. Lett.* **2007**, *91*, 053901.
3. Talaga, D.; Li, J. Single-Molecule Protein Unfolding in Solid State Nanopores. *J. Am. Chem. Soc.* **2009**, *131*, 9287–9297.
4. Freedman, K. J.; Haq, S. R.; Edel, J. B.; Jemth, P.; Kim, M. J. Single Molecule Unfolding and Stretching of Protein Domains inside a Solid-State Nanopore by Electric Field. *Sci. Rep.* **2013**, 3.
5. Wei, R.; Gatterdam, V.; Wieneke, R.; Tampé, R.; Rant, U. Stochastic Sensing of Proteins with Receptor-Modified Solid-State Nanopores. *Nat. Nanotechnol.* **2012**, *7*, 257–263.
6. Freedman, K. J.; Bastian, A. R.; Chaiken, I.; Kim, M. J. Solid-State Nanopore Detection of Protein Complexes: Applications in Healthcare and Protein Kinetics. *Small* **2013**, *9*, 750–759.
7. Han, A.; Creus, M.; Schürmann, G.; Linder, V.; Ward, T. R.; de Rooij, N. F.; Staufer, U. Label-Free Detection of Single Protein Molecules and Protein−Protein Interactions Using Synthetic Nanopores. *Anal. Chem.* **2008**, *80*, 4651–4658.
8. Yusko, E.; Johnson, J.; Majd, S.; Prangkio, P.; Rollings, R.; Li, J.; Yang, J.; Mayer, M. Controlling Protein Translocation through Nanopores with Bio-Inspired Fluid Walls. *Nat. Nanotechnol.* **2011**, *6*, 253–260.
9. Wanunu, M.; Morrison, W.; Rabin, Y.; Grosberg, A. Y.; Meller, A. Electrostatic Focusing of Unlabelled DNA into Nanoscale Pores Using a Salt Gradient. *Nat. Nanotechnol.* **2010**, *5*, 160–165.
10. Mihovilovic, M.; Hagerty, N.; Stein, D. Statistics of DNA Capture by a Solid-State Nanopore. *Phys. Rev. Lett.* **2013**, *110*, 028102.
11. He, Y.; Tsutsui, M.; Fan, C.; Taniguchi, M.; Kawai, T. Gate Manipulation of DNA Capture into Nanopores. *ACS Nano* **2011**, *5*, 8391–8397.
12. Henrickson, S. E.; Misakian, M.; Robertson, B.; Kasianowicz, J. J. Driven DNA Transport into an Asymmetric Nanometer-Scale Pore. *Phys. Rev. Lett.* **2000**, *85*, 3057–3060.
13. Grosberg, A. Y.; Rabin, Y. DNA Capture into a Nanopore: Interplay of Diffusion and Electrohydrodynamics. *J. Chem. Phys.* **2010**, *133*, 165102.
14. Pastoriza-Gallego, M.; Rabah, L.; Gibrat, G.; Thiebot, B.; van der Goot, F. G.; Auvray, L.; Betton, J.-M.; Pelta, J. Dynamics of Unfolded Protein Transport through an Aerolysin Pore. *J. Am. Chem. Soc.* **2011**, *133*, 2923–2931.
15. Oukhaled, A.; Cressiot, B.; Bacri, L.; Pastoriza-Gallego, M.; Betton, J.-M.; Bourhis, E.; Jede, R.; Gierak, J.; Auvray, L. c.; Pelta, J. Dynamics of Completely Unfolded and Native Proteins through Solid-State Nanopores as a Function of Electric Driving Force. *ACS Nano* **2011**, *5*, 3628–3638.
16. Miles, B.; Ivanov, A.; Wilson, K.; Dogan, F.; Japrung, D.; Edel, J. Single Molecule Sensing with Solid-State Nanopores: Novel Materials, Methods, and Applications. *Chem. Soc. Rev.* **2013**, *42*, 15–28.
17. Cheley, S.; Xie, H.; Bayley, H. A Genetically Encoded Pore for the Stochastic Detection of a Protein Kinase. *ChemBioChem* **2006**, *7*, 1923–1927.
18. Cressiot, B.; Oukhaled, A.; Patriarche, G.; Pastoriza-Gallego, M.; Betton, J.-M.; Auvray, L.; Muthukumar, M.; Bacri, L.; Pelta, J. Protein Transport through a Narrow Solid-State Nanopore at High Voltage: Experiments and Theory. *ACS Nano* **2012**, *6*, 6236–6243.
19. Japrung, D.; Dogan, J.; Freedman, K. J.; Nadzeyka, A.; Bauerdick, S.; Albrecht, T.; Kim, M. J.; Jemth, P.; Edel, J. B. Single-Molecule Studies of Intrinsically Disordered Proteins Using Solid-State Nanopores. *Anal. Chem.* **2013**, *85*, 2449–2456.
20. Siwy, Z.; Trofin, L.; Kohli, P.; Baker, L. A.; Trautmann, C.; Martin, C. R. Protein Biosensors Based on Biofunctionalized Conical Gold Nanotubes. *J. Am. Chem. Soc.* **2005**, *127*, 5000–5001.
21. Li, W.; Bell, N. A. W.; Hernández-Ainsa, S.; Thacker, V. V.; Thackray, A. M.; Bujdoso, R.; Keyser, U. F. Single Protein Molecule Detection by Glass Nanopores. *ACS Nano* **2013**, *7*, 4129–4134.

22. Larkin, J.; Henley, R. Y.; Muthukumar, M.; Rosenstein, J. K.; Wanunu, M. High-Bandwidth Protein Analysis Using Solid-State Nanopores. *Biophys. J.* **2014**, *106*, 696–704.
23. Rotem, D.; Jayasinghe, L.; Salichou, M.; Bayley, H. Protein Detection by Nanopores Equipped with Aptamers. *J. Am. Chem. Soc.* **2012**, *134*, 2781–2787.
24. Merstorf, C. L.; Cressiot, B.; Pastoriza-Gallego, M.; Oukhaled, A.; Betton, J.-M.; Auvray, L.; Pelta, J. Wild Type, Mutant Protein Unfolding and Phase Transition Detected by Single-Nanopore Recording. *ACS Chem. Biol.* **2012**, *7*, 652–658.
25. Singh, P. R.; Bárcena-Uribarri, I.; Modi, N.; Kleinekathöfer, U.; Benz, R.; Winterhalter, M.; Mahendran, K. R. Pulling Peptides across Nanochannels: Resolving Peptide Binding and Translocation through the Hetero-Oligomeric Channel from *Nocardia farcinica*. *ACS Nano* **2012**, *6*, 10699–10707.
26. Wanunu, M.; Bhattacharya, S.; Xie, Y.; Tor, Y.; Aksimentiev, A.; Drndic, M. Nanopore Analysis of Individual RNA/Antibiotic Complexes. *ACS Nano* **2011**, *5*, 9345–9353.
27. Hornblower, B.; Coombs, A.; Whitaker, R. D.; Kolomeisky, A.; Picone, S. J.; Meller, A.; Akeson, M. Single-Molecule Analysis of DNA−Protein Complexes Using Nanopores. *Nat. Methods* **2007**, *4*, 315–317.
28. Galla, L.; Meyer, A. J.; Spiering, A.; Sischka, A.; Mayer, M.; Hall, A. R.; Reimann, P.; Anselmetti, D. Hydrodynamic Slip on DNA Observed by Optical Tweezers-Controlled Translocation Experiments with Solid-State and Lipid-Coated Nanopores. *Nano Lett.* **2014**, *14*, 4176–4182.
29. Wang, D.; Harrer, S.; Luan, B.; Stolovitzky, G.; Peng, H.; Afzali-Ardakani, A. Regulating the Transport of DNA through Biofriendly Nanochannels in a Thin Solid Membrane. *Sci. Rep.* **2014**, 4.
30. Soskine, M.; Biesemans, A.; De Maeyer, M.; Maglia, G. Tuning the Size and Properties of ClyA Nanopores Assisted by Directed Evolution. *J. Am. Chem. Soc.* **2013**, *135*, 13456–13463.
31. Oukhaled, A.; Bacri, L.; Pastoriza-Gallego, M.; Betton, J.-M.; Pelta, J. Sensing Proteins through Nanopores: Fundamental to Applications. *ACS Chem. Biol.* **2012**, *7*, 1935–1949.
32. Schuler, B.; Hofmann, H. Single-Molecule Spectroscopy of Protein Folding Dynamics—Expanding Scope and Timescales. *Curr. Opin. Struct. Biol.* **2013**, *23*, 36–47.
33. Kaufman, L. J. Heterogeneity in Single-Molecule Observables in the Study of Supercooled Liquids. *Annu. Rev. Phys. Chem.* **2013**, *64*, 177–200.
34. Yu, H.; Liu, X.; Neupane, K.; Gupta, A. N.; Brigley, A. M.; Solanki, A.; Sosova, I.; Woodside, M. T. Direct Observation of Multiple Misfolding Pathways in a Single Prion Protein Molecule. *Proc. Natl. Acad. Sci. U.S.A.* **2012**, *109*, 5283–5288.
35. Arai, M.; Ferreon, J. C.; Wright, P. E. Quantitative Analysis of Multisite Protein−Ligand Interactions by NMR: Binding of Intrinsically Disordered p53 Transactivation Subdomains with the TAZ2 Domain of CBP. *J. Am. Chem. Soc.* **2012**, *134*, 3792–3803.
36. Boehr, D. D.; Nussinov, R.; Wright, P. E. The Role of Dynamic Conformational Ensembles in Biomolecular Recognition. *Nat. Chem. Biol.* **2009**, *5*, 789–796.
37. Lange, O. F.; Lakomek, N.-A.; Farès, C.; Schröder, G. F.; Walter, K. F.; Becker, S.; Meiler, J.; Grubmüller, H.; Griesinger, C.; De Groot, B. L. Recognition Dynamics up to Microseconds Revealed from an RDC-Derived Ubiquitin Ensemble in Solution. *Science* **2008**, *320*, 1471–1475.
38. Sexton, L. T.; Mukaibo, H.; Katira, P.; Hess, H.; Sherrill, S. A.; Horne, L. P.; Martin, C. R. An Adsorption-Based Model for Pulse Duration in Resistive-Pulse Protein Sensing. *J. Am. Chem. Soc.* **2010**, *132*, 6755–6763.
39. Niedzwiecki, D. J.; Grazul, J.; Movileanu, L. Single-Molecule Observation of Protein Adsorption onto an Inorganic Surface. *J. Am. Chem. Soc.* **2010**, *132*, 10816–10822.
40. Stellwagen, N.; Gelfi, C.; Righetti, P. The Free Solution Mobility of DNA. *Biopolymers* **1997**, *42*, 687–703.
41. Heng, J.; Ho, C.; Kim, T.; Timp, R.; Aksimentiev, A.; Grinkova, Y.; Sligar, S.; Schulten, K.; Timp, G. Sizing DNA Using a Nanometer-Diameter Pore. *Biophys. J.* **2004**, *87*, 2905–2911.
42. Kasianowicz, J.; Brandin, E.; Branton, D.; Deamer, D. Characterization of Individual Polynucleotide Molecules Using a Membrane Channel. *Proc. Natl. Acad. Sci. U.S.A.* **1996**, *93*, 13770–13773.
43. Oukhaled, G.; Mathé, J.; Biance, A. L.; Bacri, L.; Betton, J. M.; Lairez, D.; Pelta, J.; Auvray, L. Unfolding of Proteins and Long Transient Conformations Detected by Single Nanopore Recording. *Phys. Rev. Lett.* **2007**, *98*, 158101.
44. Plesa, C.; Kowalczyk, S. W.; Zinsmeester, R.; Grosberg, A. Y.; Rabin, Y.; Dekker, C. Fast Translocation of Proteins through Solid State Nanopores. *Nano Lett.* **2013**, *13*, 658–663.
45. Talaga, D. S.; Li, J. Single-Molecule Protein Unfolding in Solid State Nanopores. *J. Am. Chem. Soc.* **2009**, *131*, 9287–9297.
46. Arai, T.; Norde, W. The Behavior of Some Model Proteins at Solid−Liquid Interfaces. *Colloids Surf.* **1990**, *51*, 1–15.
47. Firnkes, M.; Pedone, D.; Knezevic, J.; Döblinger, M.; Rant, U. Electrically Facilitated Translocations of Proteins through Silicon Nitride Nanopores: Conjoint and Competitive Action of Diffusion, Electrophoresis, and Electroosmosis. *Nano Lett.* **2010**, *10*, 2162–2167.
48. Prabhu, A. S.; Jubery, T. Z. N.; Freedman, K. J.; Mulero, R.; Dutta, P.; Kim, M. J. Chemically Modified Solid State Nanopores for High Throughput Nanoparticle Separation. *J. Phys.: Condens. Matter* **2010**, *22*, 454107.
49. Gasteiger, E.; Hoogland, C.; Gattiker, A.; Wilkins, M. R.; Appel, R. D.; Bairoch, A. Protein Identification and Analysis Tools on the Expasy Server. In *The Proteomics Protocols Handbook*; Springer: Berlin, 2005; pp 571−607.
50. Ivarsson, Y. Plasticity of PDZ Domains in Ligand Recognition and Signaling. *FEBS Lett.* **2012**, *586*, 2638–2647.
51. Chi, C. N.; Bach, A.; Engström, Å.; Wang, H.; Strømgaard, K.; Gianni, S.; Jemth, P. A Sequential Binding Mechanism in a PDZ Domain. *Biochemistry* **2009**, *48*, 7089–7097.
52. Haq, S. R.; Jürgens, M. C.; Chi, C. N.; Koh, C.-S.; Elfström, L.; Selmer, M.; Gianni, S.; Jemth, P. The Plastic Energy Landscape of Protein Folding. *J. Biol. Chem.* **2010**, *285*, 18051–18059.
53. Kannam, S. K.; Kim, S. C.; Rogers, P. R.; Gunn, N.; Wagner, J.; Harrer, S.; Downton, M. T. Sensing of Protein Molecules through Nanopores: A Molecular Dynamics Study. *Nanotechnology* **2014**, *25*, 155502.
54. van Dorp, S.; Keyser, U. F.; Dekker, N. H.; Dekker, C.; Lemay, S. G. Origin of the Electrophoretic Force on DNA in Solid-State Nanopores. *Nat. Phys.* **2009**, *5*, 347–351.
55. Harjinder Singh, H.; Karlapalem, K.; Mitra, A. A Real Valued Genetic Algorithm for Generating Native Like Structure of Small Globular Protein. *IEEE Eng. Med. Biol. Soc.* **2008**, 1359–1362.
56. Kohn, J. E.; Millett, I. S.; Jacob, J.; Zagrovic, B.; Dillon, T. M.; Cingel, N.; Dothager, R. S.; Seifert, S.; Thiyagarajan, P.; Sosnick, T. R. Random-Coil Behavior and the Dimensions of Chemically Unfolded Proteins. *Proc. Natl. Acad. Sci. U.S.A.* **2004**, *101*, 12491–12496.
57. Zhou, H. Influence of Crowded Cellular Environments on Protein Folding, Binding, and Oligomerization: Biological Consequences and Potentials of Atomistic Modeling. *FEBS Lett.* **2013**, *587*, 1053–1061.
58. Zhou, H. X. Protein Folding and Binding in Confined Spaces and in Crowded Solutions. *J. Mol. Recognit.* **2004**, *17*, 368–375.
59. Shtilerman, M. D.; Ding, T. T.; Lansbury, P. T. Molecular Crowding Accelerates Fibrillization of α-Synuclein: Could an Increase in the Cytoplasmic Protein Concentration Induce Parkinson's Disease? *Biochemistry* **2002**, *41*, 3855–3860.
60. Soranno, A.; Koenig, I.; Borgia, M. B.; Hofmann, H.; Zosel, F.; Nettels, D.; Schuler, B. Single-Molecule Spectroscopy Reveals Polymer Effects of Disordered Proteins in Crowded Environments. *Proc. Natl. Acad. Sci. U.S.A.* **2014**, *111*, 4874–4879.
61. Zhou, H.-X. Polymer Crowders and Protein Crowders Act Similarly on Protein Folding Stability. *FEBS Lett.* **2013**, *587*, 394–397.
62. Batra, J.; Xu, K.; Qin, S.; Zhou, H.-X. Effect of Macromolecular Crowding on Protein Binding Stability: Modest Stabilization and Significant Biological Consequences. *Biophys. J.* **2009**, *97*, 906–911.